Thin-Walled Structures 137 (2019) 515–526

Contents lists available at ScienceDirect

Thin-Walled Structures

journal homepage: www.elsevier.com/locate/tws

Full length article

Improving buckling resistance of hollow structural steel columns strengthened with polymer-mortar

Kh. M. El-Sayed, Ahmed S. Debaiky, Nader N. Khalil, Ibrahim M. El-Shenawy*

Department of Civil Engineering, Benha Faculty of Engineering, Benha University, Egypt

ARTICLE INFO

Keywords:
Steel
SHS
Polymer
Mortar
Column
Buckling
Strength

ABSTRACT

Experimental study is carried out to investigate the behavior and strength of square hollow structural section (SHS) columns, strengthened with an innovative polymer-mortar system. Thirteen specimens of cold-formed SHS columns with different variables are chosen. Three short-column and ten long-column SHS specimens were experimentally tested. The local and overall buckling of specimens are measured in the laboratory. The tested specimens are subjected to an axial compressive load. The effect of the thickness of polymer-mortar applied directly to the well-prepared steel surface was studied. The effect of slenderness ratio *(kL/r)* and width-to-thickness ratio *(b/t)* on the effectiveness of mortar strengthening was also discussed. Different failure modes are discussed as well as complete axial strength curves are drawn for different cross-sections and member lengths. A maximum axial strength gain of 31.6% was achieved for SHS short columns strengthened with 6 mm thickness polymer-mortar layer. For long columns, a maximum strength gain of 76.7% was achieved with 6 mm thickness polymer-mortar layer applied on four sides. In all mortar-strengthened SHS short and long columns, the axial and lateral deflection, and the axial strain were reduced. The axial strength of SHS long slender columns increased greatly as the overall slenderness ratio increases.

1. Introduction

The use of cold-formed steel members is economical alternative in design for low-rise buildings compared to hot-rolled steel members. As a result of their advantages such as high strength-to-weight ratio, flexible section shapes, easy to fabricate, transport, and erect, recycle etc. Steel square hollow sections (SHS) are used widely in many structural forms in engineering applications. SHS are produced in compact, non-compact and slender geometries (defined by the appropriate international steel specification). Two types of buckling modes may occur in compression steel elements - namely - local buckling, that occurs within the thin elements comprising the cross section of a member, and overall buckling that takes place in slender compression members. When a cold-formed column is under compressive loading, component plates of the member usually buckle prior to overall failure. The major effect of local buckling is the reduction of the member stiffness against overall bending and/or torsion. This is the main factor that causes the early failure of the column, and decreases the loading capacity of the member considerably, Jaehong Lee et al. [4]. The local buckling failure mode is mainly affected by plate slenderness ratio (flat width – to – thickness ratio) of the section. The overall buckling failure mode is mainly affected by slenderness ratio of the member as well as the section width – to – thickness ratio, [3].

Strengthening of existing steel structural members is needed due to some reasons. It may be required because of an inadequate design, damage, fatigue cracking, or deterioration such as corrosion, or to increase the structure capability to carry excessive loads. Bonding FRP composites to steel surfaces has been developed as a successive approach to strengthen steel members instead of other conventional methods using steel plating to improve fatigue life, durability and load-bearing capacity. Recent investigations on thin-walled steel sections strengthened with Fiber Reinforced Polymer (FRP) were presented by researchers [5–18]. Wrapping of steel columns with FRP composites is the most commonly used method of retrofitting to increase their load capacity. The researchers showed the behavior of members in terms of load-deflection, load-strain, modes of failure, and structural ductility. Despite these features, there are some disadvantages to these FRP composites. The disadvantages are their high initial costs, susceptibility to mechanical damage and fire resistance, poor shear strength and low strain to failure. One more disadvantage of CFRP Composites is that more brittle than wrought metals and thus are more easily damaged. In addition, methods to enhance the buckling resistance of cold-formed steel members in compression have not yet been fully studied.

In the field of Materials Science and Engineering (MSE) concrete

* Corresponding author.
E-mail address: ibrahim.alshenawi@bhit.bu.edu.eg (I.M. El-Shenawy).

https://doi.org/10.1016/j.tws.2018.12.029
Received 13 July 2018; Received in revised form 4 November 2018; Accepted 19 December 2018
0263-8231/ © 2018 Elsevier Ltd. All rights reserved.

Table 1
Summary of compressive strength and Push-out tests on SIKADUR-41 CF.

Mixture	Specimen	SIKADUR-41 CF			Compressive Strength Test		Push-out Test	
		Epoxy Content (%)		Sand Content (%)	P_{max} (kN)	Compressive Strength (MPa)	P_{max} (kN)	Bond Strength (MPa)
		Resin	Hardener					
Mix − 1	M1-A	26.67	13.33	60	150.3	60.1	77.19	1.93
	M1-B				146.5	58.6	83.22	2.08
	Average					**59.35**		**2.00**
Mix − 2	M2-A	33.33	16.67	50	160.5	64.2	117.89	2.95
	M2-B				164.7	65.9	119.55	2.99
	Average					**65.05**		**2.97**
Mix − 3	M3-A	40	20	40	146	58.4	108.04	2.70
	M3-B				145.3	58.1	111.79	2.79
	Average					**58.25**		**2.75**

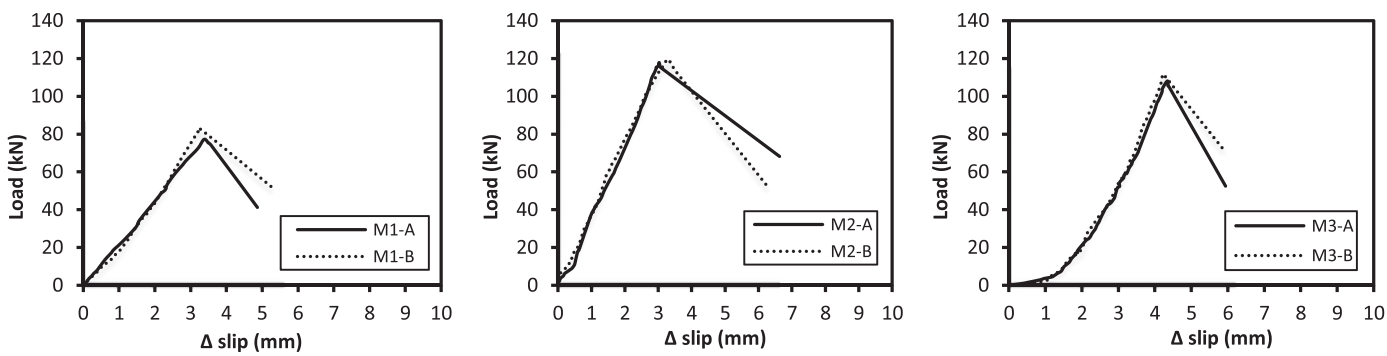

Fig. 1. Push-out test relationships.

and polymer have been familiar materials. In the last decade, technological investigations concerning modifications of concrete by polymeric materials have been conducted. Such composite materials are known as polymer concrete (PCt) and possesses several advantages such as higher strength and a shorter curing process. Knowledge of so-called polymer concrete has significantly progressed since 1960. Modifying cement formulations with polymers provides many important properties that make a variety of niche applications possible, including concrete patch and repair. In this study, polymer mortar is a composite material formed by combining mineral aggregates (fine sand) with a monomer, usually of a thermoset polymer resin. Typically polymer mortar possesses also other advantages compared to regular mortar such as: bond strength, increased freeze-thaw resistance, high abrasion resistance, increased flexural, compressive and tensile strengths, good durability, improved chemical resistance in harsh environments. Moreover, they exhibit good creep resistance, and high UV resistance due to the very low polymer content and inert fillers. El-Tawil and Ekiz [18] proposed a new strengthening method of steel bracing using mortar, in which mortar blocks were attached around single angle and double angle braces with FRP sheets wrapped outside, and the maximum compressive load was increased from 52% to 200% after strengthening. Liu et al. [19] presented the experimental and analytical results of a retrofitting method, in which FRP jackets were wrapped around corroded steel columns only within the corroded zone, and subsequently filled with lightweight concrete. The strengthened specimens failed through global buckling with an increase of load-bearing capacity of 58–233%, which was still much lower than the yielding capacity of the full section. Feng et al. [20] improved a strengthening approach to the buckling resistance of steel members in compression, where a mortar-filled FRP tube is sleeved outside the steel member and wrapped with FRP fabrics at the ends of the tube. It was found that, after strengthening, the failure modes changed from steel yielding at the mid-height of the steel member due to global buckling to local damage at the steel end. As a result, the load bearing capacity increased by 44–215% and ductility increased by up to 877%. As a result of recent researches on polymer-mortar as well as the advantages of these materials such as: good bond strength, fire resistance, improved chemical resistance, and increased flexural and compressive strengths, Moreover, the ease of application to the outer surface of steel members to increase the cross section area, the authors thought about using these materials to strengthen the thin-walled steel sections.

The main objective of this study is to explore an innovative strengthening system to improve the buckling resistance of steel cold-formed SHS columns under axial concentric loading. The strengthening technique depends on the use of a polymeric light weight, high strength and low cost strengthening materials, namely, polymer-mortar bonded directly to the well-prepared steel surface. To understand the effectiveness of this strengthening system. Thirteen columns, 500–1853 mm length (i.e. with overall slenderness ratios ranging from 10 to 58) were experimentally tested. The parameters considered were the effect of mortar layer thickness, width-to-thickness ratio, and the overall slenderness ratio of the columns. The columns were instrumented to examine their behavior in terms of the following responses: load-axial displacement, load-lateral displacement, and load-longitudinal strains. The failure modes of the mortar-strengthened specimens were discussed in comparison to the unstrengthened reference specimens.

2. Experimental program

2.1. Materials

Polymer-mortar is a combination of epoxy resins and selected quartz aggregates. The polymer acts as an impermeable layer, ultimately leading to a stronger mortar with fewer voids. Epoxy resins in the mortar mixture offer a good adhesion to most surfaces. The density of the polymer-mortar mixture is approximately equivalent to a quarter of steel density. A solvent-free, three-components (A, B, and C), thixotropic patching and repair mortar, commercially known as SIKADUR-41

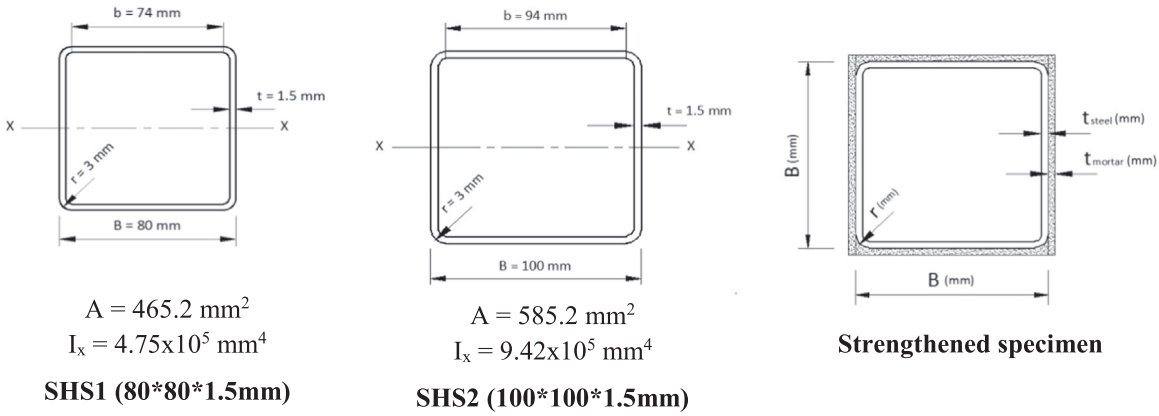

Fig. 2. SHS column's cross sections.

Table 2
Experimental Program.

Group	Column type	Specimen ID	Specimen properties				Mortar layer thickness tm (mm)
			Cross-section (b*b*t) (mm)	$\lambda_b = \frac{b}{t}$	Length (mm)	$\lambda_c = \frac{kl}{r}$	
A	Long - slender	S80L30T0	80*80*1.5	49	959	30	0
		S80L30T3					3
		S80L46T0			1470	46	0
		S80L46T3					3
		S80L46T6					6
		S80L58T0			1853	58	0
		S80L58T3					3
	Long -slender	S100L46T0	100*100*1.5	63	1845	46	0
		S100L46T3					3
		S100L46T6					6
B	Short - slender	S100L10T0	100*100*1.5	63	500	10	0
		S100L10T3					3
		S100L10T6					6

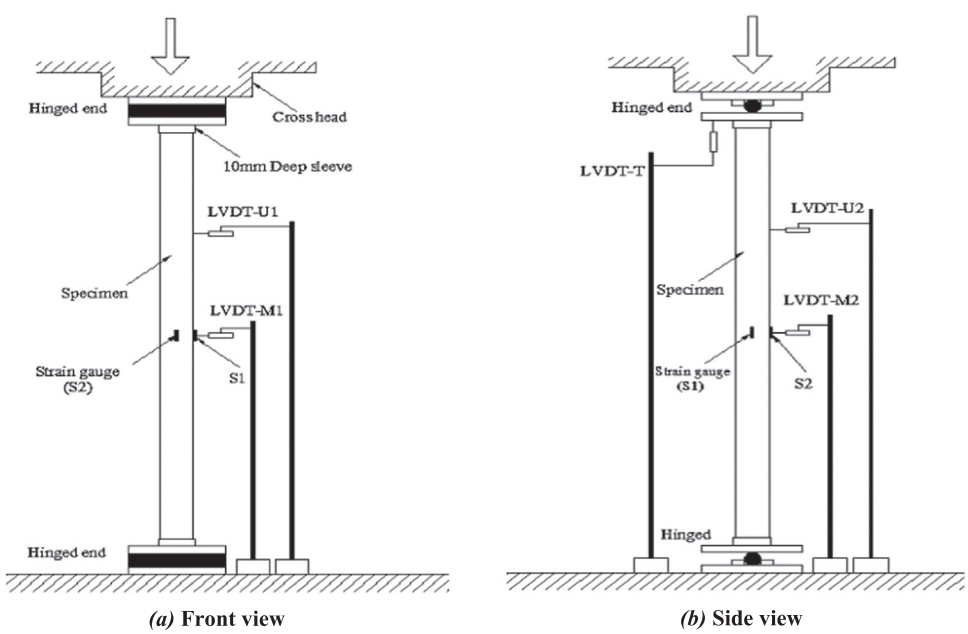

Fig. 3. Schematic view of test setup of columns in group A.

CF made by SIKA® CO branch in Swiss is used. Preliminary compressive strength and push-out tests using three different epoxy-to-filler mixtures to get the best polymer-mortar mixture were carried out as shown in Table 1. Following ASTM C39 for compressive strength test, six standard cubes were cast from the different three mix design. Two similar cubes for each polymer-mortar mixture were prepared, and kept at room temperature to the date of testing. The cubes were tested using a 2000 kN Reihle testing machine with a low rate of 1.5 kN/s. A modified push-out test is proposed to study the bond strength between polymer-mortar layer and cold-formed steel column surface. The

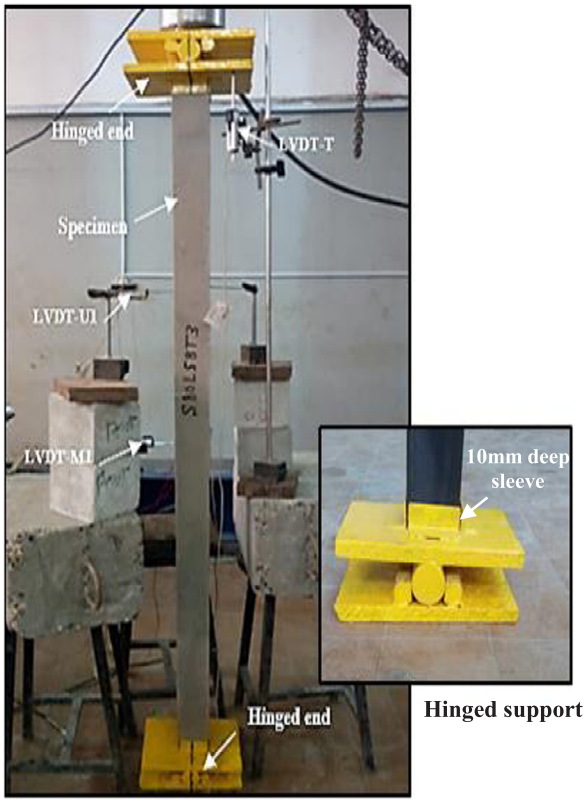

Fig. 4. Test setup of columns in group A.

modification in this test in comparison with the EC4 Standards concentrated on the use of a short piece of steel SHS column that is connected on four sides to polymer-mortar layer instead of concrete slab and steel I-Section (in Standard Push-out test) in order to be more compatible than the standard test in modeling the polymer-mortar strengthening cold-formed steel columns. The specimens are bedded down on mortar directly onto the reaction floor with load being applied to the upper end of the member. The procedure of testing was carried out in accordance with Eurocode 4 [2]. Slip between the mortar layer and the steel SHS is measured at displacement or load increments. Load-slip relationships for different polymer-mortar mixtures are shown in Fig. 1. It was concluded that Mix-2 of components mixing ratio of (A: B: C) at (2:1:3) by weight is the best mixing ratio. The behavior of Mix-2 also shows higher stiffness compared to the other mix design. Two different cross sections of cold-formed SHS, namely SHS1 and SHS2 were used to fabricate the test specimens. The two sections SHS1 and SHS2 were $80 \times 80 \times 1.5$ mm and $100 \times 100 \times 1.5$ mm, respectively. Stub-column tests are typically used in place of coupon tests to characterize the average compressive stress-strain curves for the used steel. This type of test demonstrates the overall column performance at very low slenderness ratios. Two specimens of SHS1 and SHS2 stub-columns, 120 mm and 150 mm long, respectively, were tested. Strain gauges were installed on the four sides of each stub-column to measure the longitudinal strains at mid-height of the columns. The behavior of SHS1 shows a proportional limit stress (F_p) of 180 MPa and yield strength (F_y) of 344 MPa, which indicates that the magnitude of the residual stress is approximately 48% of the yield strength. On the other hand, the behavior of SHS2 shows a proportional limit stress (F_p) of 218 MPa and yield strength (F_y) of 327 MPa, which indicates that the magnitude of residual stress is approximately 33% of the yield strength. A schematic view of the details of the tested SHS column's both cross sections is shown in Fig. 2. The design provisions of the ANSI/AISC 360-16 [1] specify the limits for the flat width-to-thickness ratio (b/t) of SHS subjected to compressive stresses equals to $(1.4 \sqrt{E/Fy})$ where F_y is the yield strength of the steel in MPa in order to permit the yielding of steel prior to local buckling under axial compression. For both SHS1 and SHS2 sections, the actual (b/t) ratios were 49.33 and 62.67, respectively, that exceeded the slenderness limit.

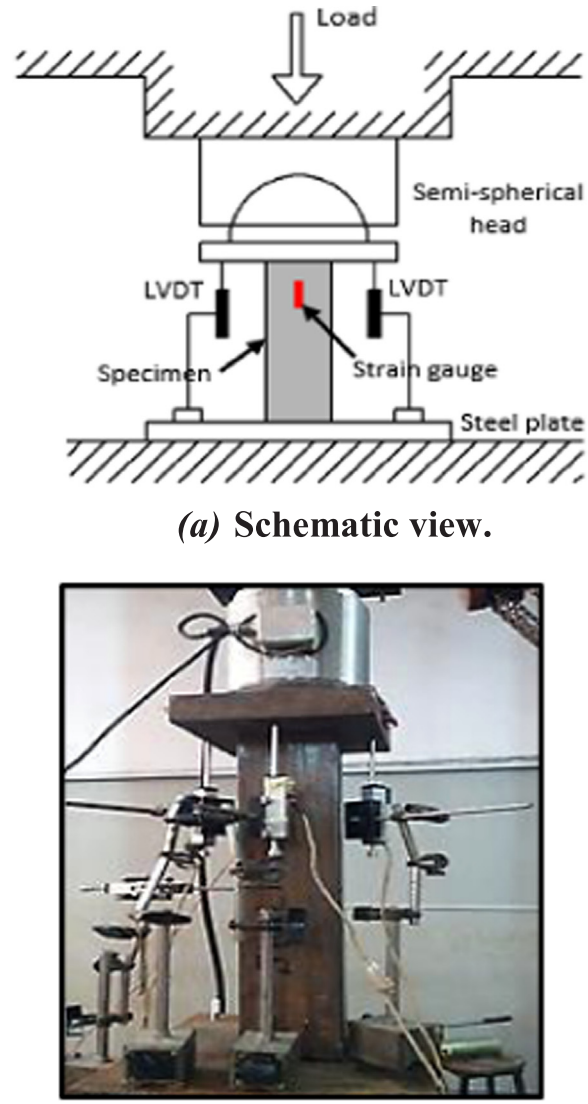

(a) **Schematic view.**

(b) **Picture of test setup.**

Fig. 5. Test setup of columns in group B.

2.2. Preparation of specimens

To examine the mentioned parameters, a total of 13 square SHS columns were experimentally tested under axial compression. The specimens were divided into two groups A, and B. Group A included long slender columns, whereas group B included short slender columns. Table 2 provides all details of the specimens, and information on strengthening scheme, including thickness of polymer-mortar. To ensure a complete bonding between the steel surface and the polymer-mortar layer, steel surface sandblasting is recommended to remove all rust, paint, and primer from the steel surface. Additionally, the bare steel surface may be pre-treated using either an adhesion promoter or a primer/conditioner, which leaves a thin layer attached to the metal oxide surface (AASHTO, 2000). The mortar layer is then applied and pressed to the pre-treated steel layer to cure for a sufficient time, not less than 48 h. The strengthened specimens were tested after mortar application by at least 10 days.

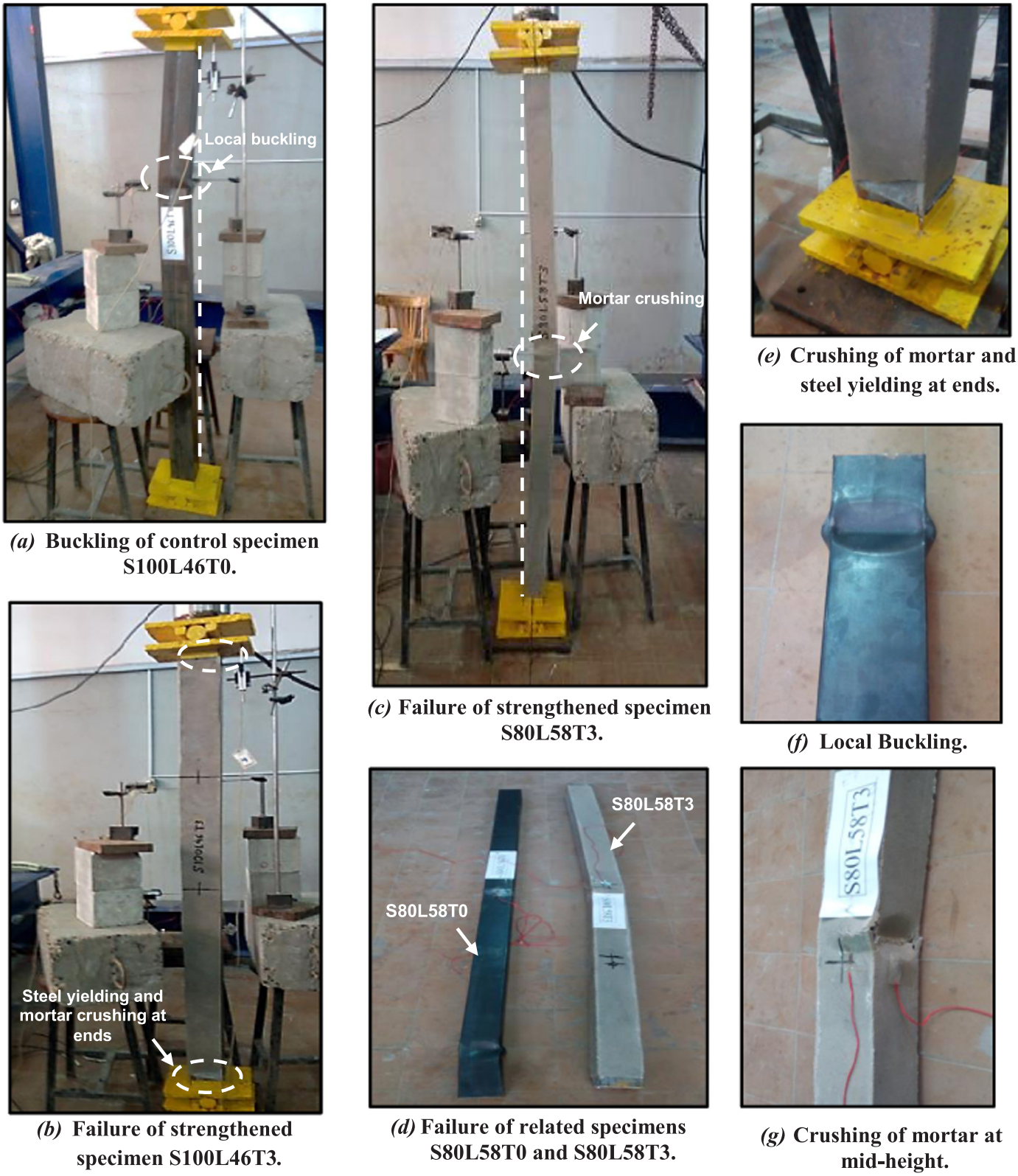

(a) **Buckling of control specimen S100L46T0.**

(b) **Failure of strengthened specimen S100L46T3.**

(c) **Failure of strengthened specimen S80L58T3.**

(d) **Failure of related specimens S80L58T0 and S80L58T3.**

(e) **Crushing of mortar and steel yielding at ends.**

(f) **Local Buckling.**

(g) **Crushing of mortar at mid-height.**

Fig. 6. Failure modes of group A columns.

2.3. Test setup and instrumentation

For columns in group A, Five LVDTs were used to measure the specimen vertical and lateral displacements. One LVDT (T) was mounted at the top of the specimen in the longitudinal direction, to measure axial displacement. Two transverse LVDTs were mounted at mid-height (M1 and M2) and quarter-points (U1 and U2) of the specimen to measure lateral displacements and capture the buckling shape. Each two transverse LVDTs were placed on adjacent sides of the specimen to express the buckling occurred both in-plane and out-of-plane direction. The longitudinal strains at mid-height of the columns were also measured using two 10 mm electric resistance strain gauges (S1

(a) **Control specimen.** *(b)* **Strengthened specimen.** *(c)* **Crushing of mortar and steel yielding at ends.**

Fig. 7. Failure modes of group B columns.

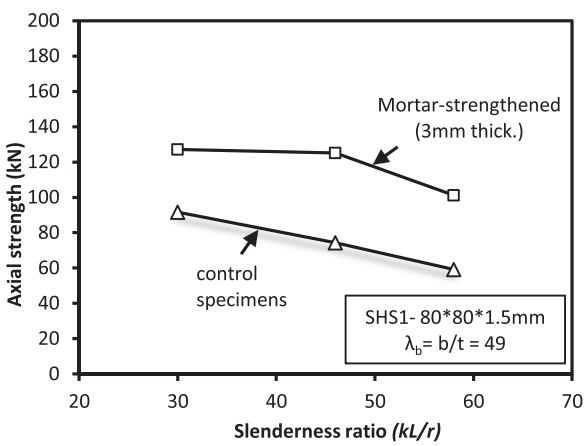

Fig. 8. Variation of axial strength with slenderness ratio of group A columns.

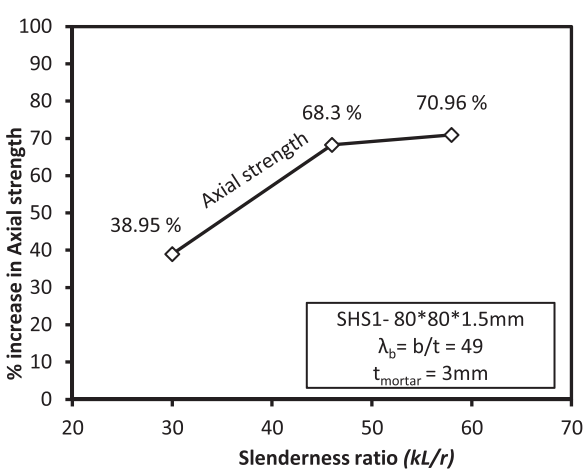

Fig. 9. Effect of slenderness ratio on mortar effectiveness in group A columns.

and S2) attached directly to the two adjacent sides of the specimens. The gauges were attached to the outer surface of the mortar layer of the strengthened columns (or to the steel surface of the control columns). All strain gauges and LVDTs are shown in Fig. 3. Prepared specimens were carefully lifted and fastened vertically to the frame test as shown in Fig. 4. The specimens were not braced against out-of-plane displacement in order to promote buckling both in-plane and out-of-plane directions. The in-plane effective length factor *(k)* for the columns tested in group A was assumed equal to 1.0 based on the permissible rotation of the end supports. For group B columns, three LVDTs were mounted around the specimen, in a vertical position, to provide a reliable average for the axial displacement of the short columns and also to check if any unintended eccentricity existed early during the test and correct the alignment accordingly. Additionally, two LVDTs were mounted at the mid-height to measure any small lateral displacements and to ensure the absence of overall buckling. 10 mm electric resistance strain gauges, installed in the longitudinal direction on two adjacent sides of the specimen, at *l/6* below the top surface, where local buckling was anticipated. Strain gauges and LVDTs were arranged and fixed as shown in Fig. 5(a), and (b). The load in this case was applied directly to a head plate on the top end of the specimen whereas the bottom end was supported by a fixed flat plate. A loading cell was mounted to monitor and control the applied loads during the test.

3. Results and discussion

3.1. Modes of failure

Literature shows that failure modes occur by local buckling and yielding at short length members, and by local flexural (overall) buckling at intermediate lengths and flexural buckling at long lengths, El Aghoury et al. [21]. In this study, the cross-section dimensions were chosen to ensure that all sections were slender. Two failure modes occurred in the tested steel cold-formed columns. In control specimens of group A, failure was mainly due to excessive overall buckling followed by local buckling for both shortest columns with slenderness ratio $kL/r = 30$, and longest columns with $kL/r = 46$ and 58 as shown in Fig. 6. This failure mode was changed in mortar-strengthened group A columns. No signs of local buckling or mortar failure by rupture or debonding have been observed. For strengthened columns with kL/r of 30 and 46, crushing of mortar layer and steel yielding were only observed at both specimen ends without any delamination or debonding from the steel surface. For the longest strengthened columns with kL/r of 58, crushing of mortar layer at mid-height without high delamination also associated with overall buckling were observed, as shown in Fig. 6(c), (d) and (g). Crushing of mortar occurred when the load was already descending, long after reaching the peak load and overall buckling has occurred. It should be noted that, this compressive failure is limited to this particular SHS section and, may vary for different SHS sections or different width-to-thickness ratios. This indicates that there was sufficient bond between steel and mortar layer to act as one unit avoiding the local buckling. This behavior also clearly suggests that the effectiveness of the polymer-mortar strengthening system increases for higher slenderness ratios.

For unstrengthened specimen of group B (S100L10T0), the typical failure mode was essentially yielding, followed by symmetric local

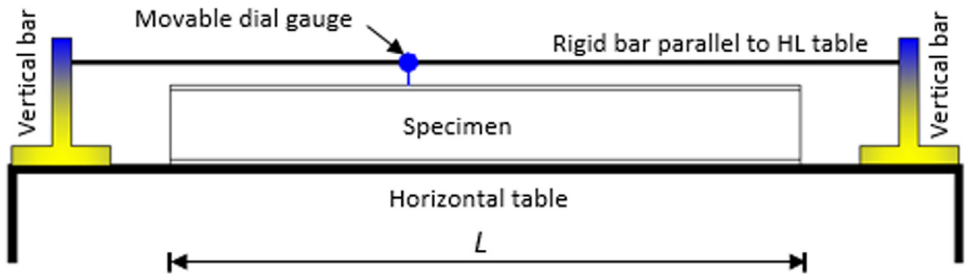

Fig. 10. Measuring of geometric imperfections.

Table 3
Geometric imperfections measurements.

Specimen	L (mm)	Side A		Side B	
		Out-of-straightness (e_{max}'- e'_{mid}) (mm)	L/e'_{max}	Out-of-straightness (e_{max}'- e'_{mid}) (mm)	L/e'_{max}
S80L30T0	959	0.92–0.74	1042	0.41–0.33	2339
S80L30T3	959	0.87 – 0.84	1102	0.42 – 0.37	2283
S80L46T0	1470	0.89–0.81	1652	0.41–0.37	3585
S80L46T3	1470	0.92 – 0.86	1598	0.46 – 0.40	3196
S80L46T6	1470	0.97 – 0.92	1515	0.53 – 0.52	2774
S80L58T0	1853	0.98 – 0.87	1891	0.53 – 0.44	3496
S80L58T3	1853	0.96–0.91	1930	0.49 – 0.48	3782
S100L46T0	1845	0.53 – 0.43	3481	0.38 – 0.33	4855
S100L46T3	1845	0.54 – 0.48	3417	0.40 – 0.35	4612
S100L46T6	1845	0.54–0.50	3417	0.39 – 0.38	4731
S100L10T0	500	0.54 – 0.53	926	0.32 – 0.32	1563
S100L10T3	500	0.58 – 0.54	862	0.34 – 0.33	1471
S100L10T6	500	0.59 – 0.56	847	0.35 – 0.35	1429

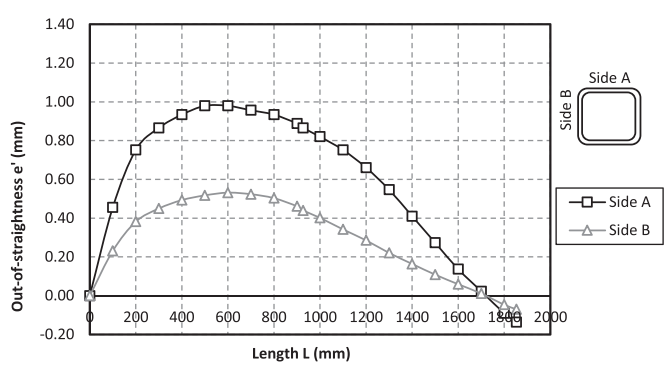

Fig. 11. Typical overall imperfection profile of specimen S80L58T0.

buckling, where two opposite faces would buckle inwards and the other two faces would buckle outwards, as shown in Fig. 7(a). In mortar-strengthened group B columns, crushing or debonding occurred between mortar layer and steel surface as well as steel yielding was only observed at both ends of the specimens without any delamination, as shown in Fig. 7(b), and (c). No local buckling was observed in the mortar-strengthened short slender columns.

3.2. Effect of overall slenderness ratio

To study the effect of slenderness ratio on effectiveness of mortar strengthening system, six specimens of group A having slenderness ratios *(kL/r)* of 30, 46, and 58 were compared. The first set of each pair is the control specimen, namely S80L30T0, S80L46T0, and S80L58T0, while the second set is the strengthened using polymer-mortar of 3 mm thickness, namely S80L30T3, S80L46T3, and S80L58T3. One of the most important criteria for the success of any strengthening technique of structural elements is the increase in ultimate load capacity. The variation of the axial strength of the control and the mortar-strengthened columns with slenderness ratio is shown in Fig. 8. It was shown that the axial strength of the control specimens reduces as the slenderness ratio increases as anticipated according to the Euler's equation. The figure also shows that, the axial strength of the mortar-strengthened specimens reduced as the slenderness ratio increases but at a much lower rate than that of the control specimens. To summarize the effect of slenderness ratio, Fig. 9 clearly demonstrates the effectiveness of the polymer-mortar strengthening system, reflected by the percentage increase in axial strength, as the slenderness ratio increases. The stability of the mortar-strengthened columns against axial shortening is improved. Applying polymer-mortar on steel cold-formed columns decreases the axial displacement compared to control specimens. It was also concluded that, the axial stiffness of SHS slender columns is also increased by using polymer-mortar strengthening materials. The behavior of mortar-strengthened specimen shows higher strength and stiffness, compared to the control specimen, which indicates that the

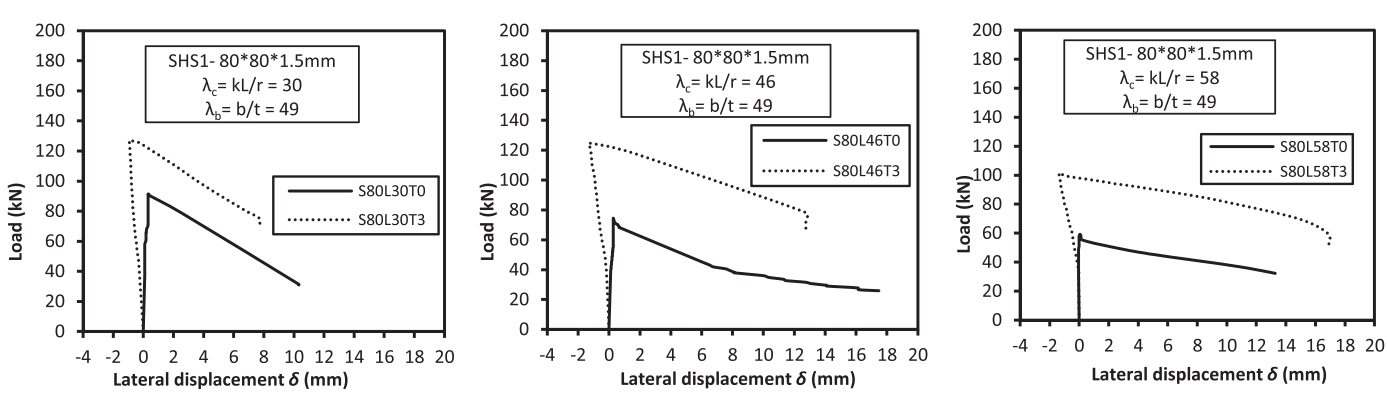

(a) kL/r = 30 (c) *kL/r = 46* (d) *kL/r = 58*

Fig. 12. Load-lateral displacement at mid-height in-plane responses of group A columns.

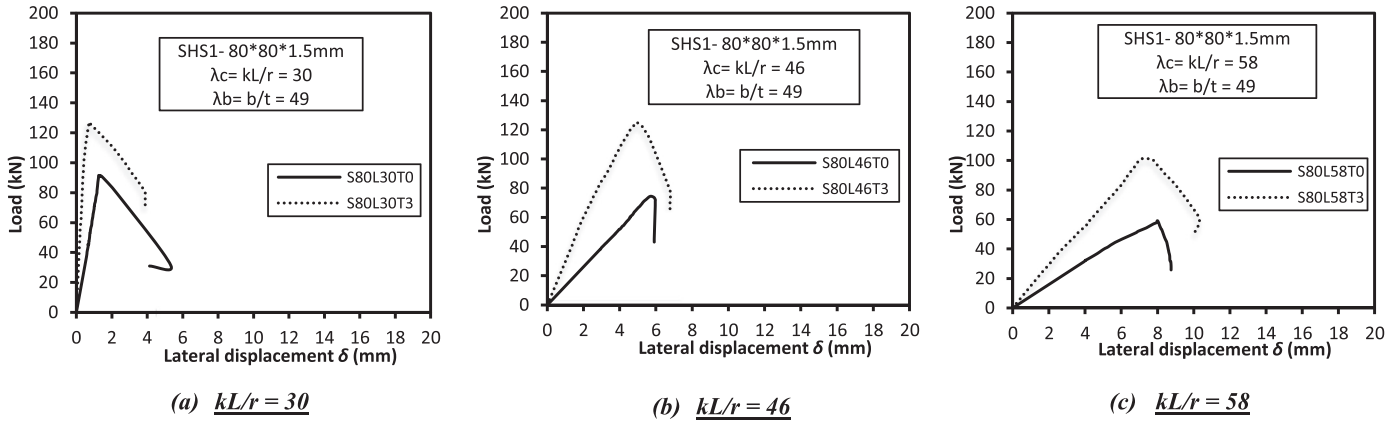

(a) kL/r = 30 *(b) kL/r = 46* *(c) kL/r = 58*

Fig. 13. Load-lateral displacement at mid-height out-of-plane responses of group A columns.

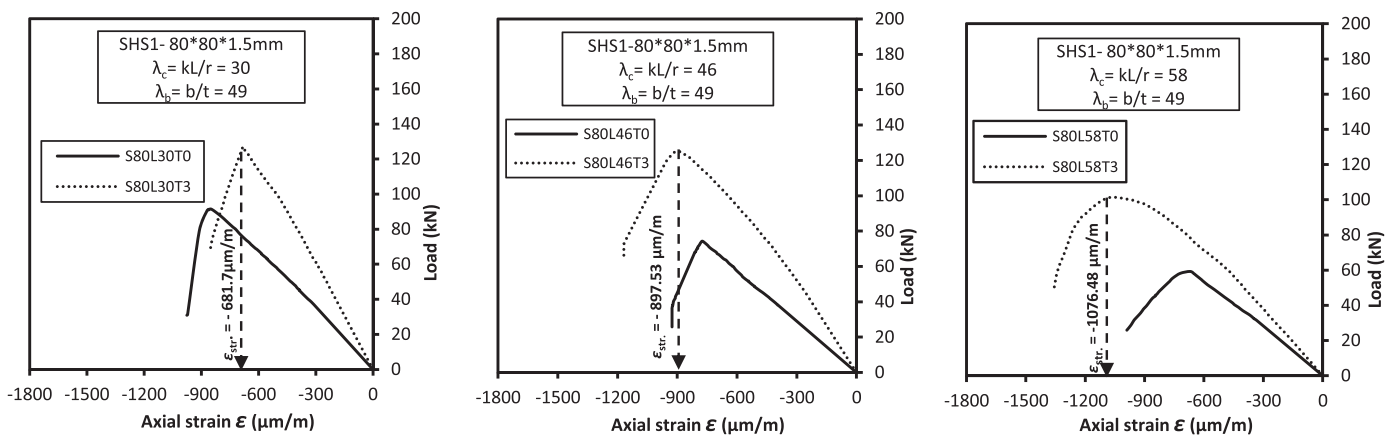

(a) kL/r = 30 *(b) kL/r =46* *(c) kL/r =58*

Fig. 14. Load-axial strain in-plane responses of group A columns.

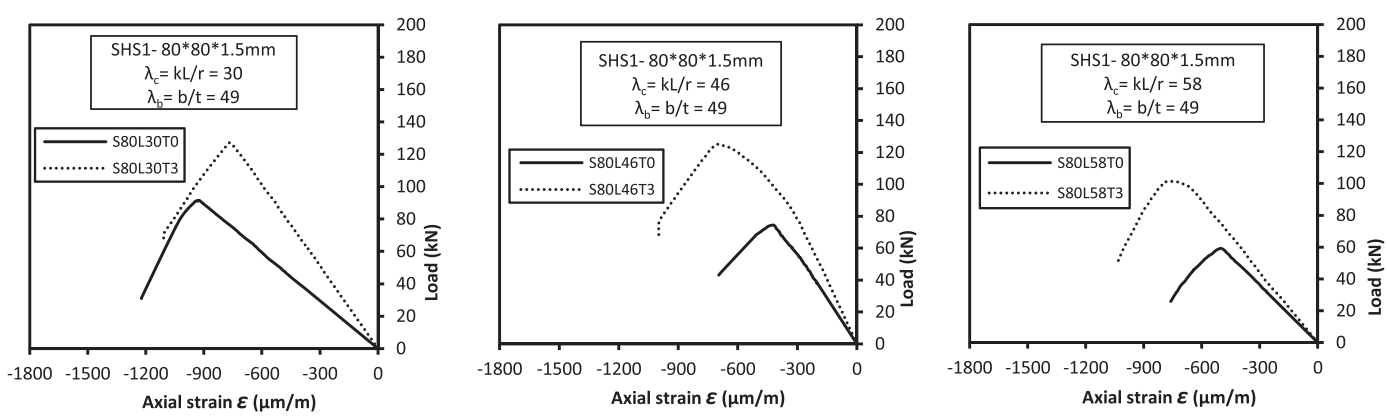

(a) kL/r = 30 *(b) kL/r = 46* *(c) kL/r = 58*

Fig. 15. Load-axial strain out-of-plane responses of group A columns.

polymer-mortar has improved the stability of the column against axial and lateral deflections.

During the rolling and cooling manufacturing processes of the steel cold-formed sections, the steel sections produced can never be perfectly straight. Generally, the geometric imperfections are divided into two main categories; cross-sectional imperfections and global imperfections. The cross-sectional imperfections represent the out of the flatness of the plate elements forming the sections, however, the overall imperfections are defined as the out of straightness along the member axis. For any elastic pin-ended long slender column, there is a slight initial curvature due to out of straightness of amplitude e′ at mid-height. As the column is loaded, it deflects further and the additional lateral displacement at mid-height is δ. In this study, thirteen SHS specimens were prepared for measuring the geometric imperfections. The same 13 SHS specimens were tested under axial compressive loading. To measure the geometric imperfections, the specimens were placed on a completely horizontal table. A movable dial gauge with an accuracy of ± 0.01 mm was used to measure the imperfections. The dial gauge move along a rigid bar

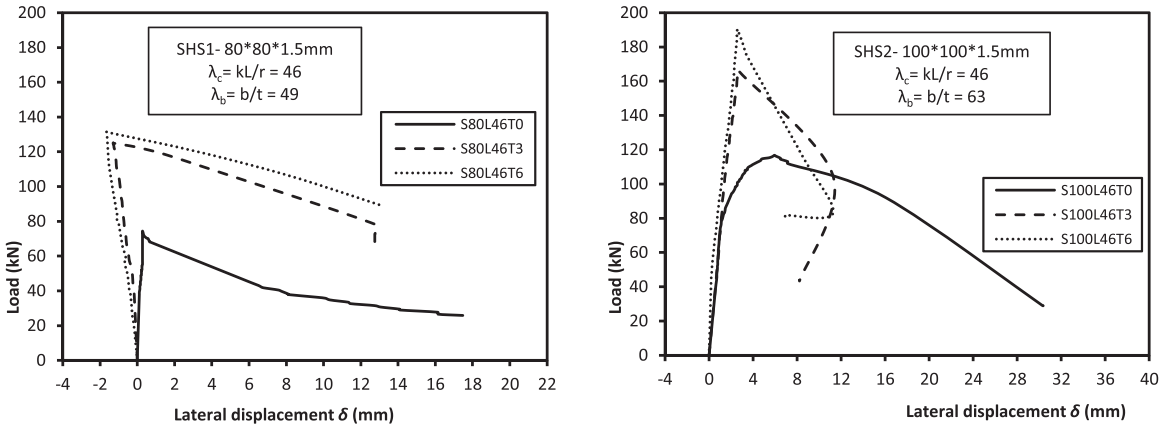

(a) ***SHS1*** *(b)* ***SHS2***

Fig. 16. Effect of section's geometry on lateral displacement in-plane at mid-height.

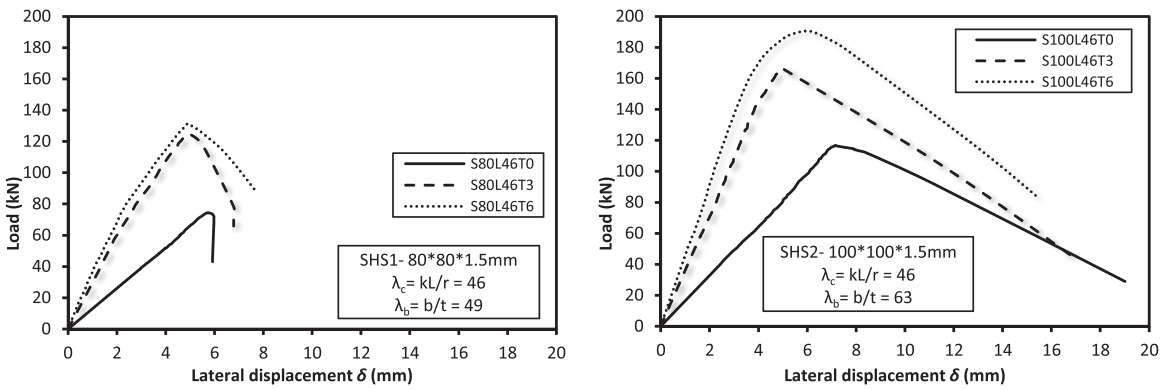

(a) ***SHS1*** *(b)* ***SHS2***

Fig. 17. Effect of section's geometry on lateral displacement out-of-plane at mid-height.

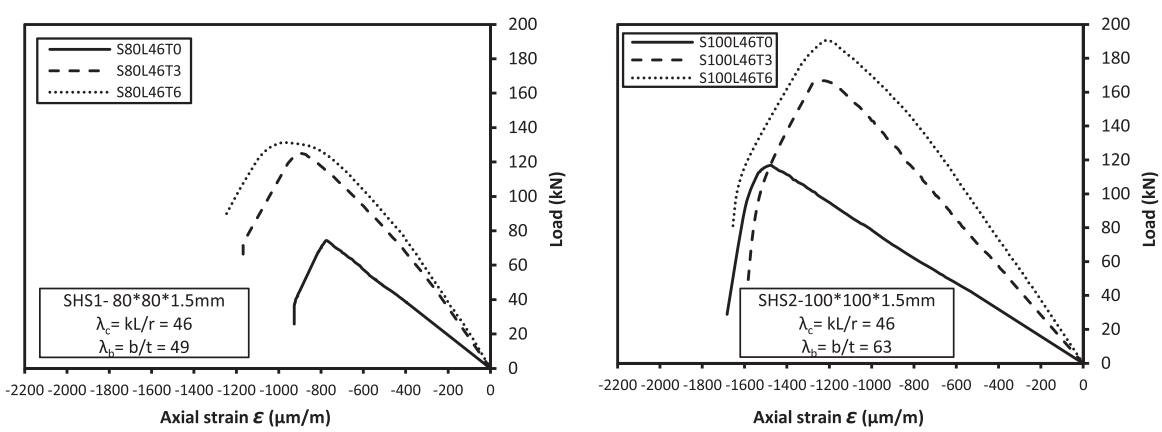

(a) ***SHS1*** *(b)* ***SHS2***

Fig. 18. Effect of section's geometry on axial strain in-plane.

fixed exactly parallel to the table as shown in Fig. 10. Readings were taken for equally spaced 6 sections along the member length. In each section, measurements were done for 10 points. Each section was 100 mm length and measurements were done for 10 points. The measured out-of-straightness, e', as well as, the frequencies of the overall imperfections, L/e', in both sides are listed in Table 3. It was found that, the out-of-straightness varied from L/4855 to L/847 and the highest frequency value was L/1891. It is worth noted that, the limit of measured values for the overall geometric imperfections for eight lipped sigma sections specimens obtained by El Aghoury et al., (2014), varied from L/3500 to L/890. For overall imperfections, typically L/1000 is used as the initial geometric imperfection value based on ANSI/AISC 303, where L is the member length between brace or framing points. The overall geometric imperfections of specimen S80L58T0 is shown in Fig. 11. As stated earlier, no lateral supports were used. Under axial loading, the long columns deform both in-plane and out-of-plane direction. As shown in Fig. 12 related to LVDT-M2 measurements, the small values of lateral displacement up to the peak load are a result of

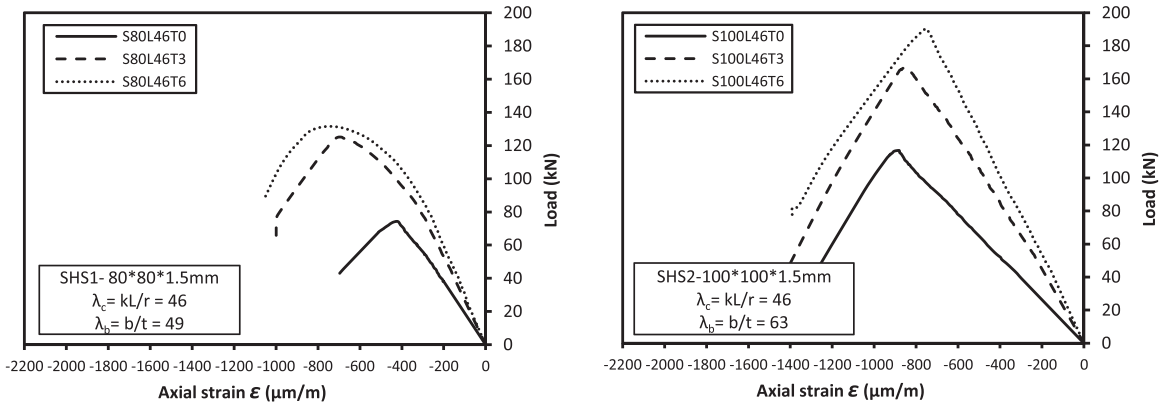

(a) ***SHS1*** *(b)* ***SHS2***

Fig. 19. Effect of section's geometry on axial strain out-of-plane.

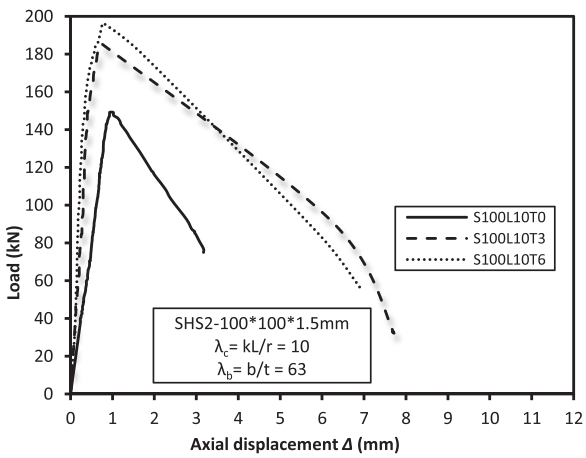

Fig. 20. Load-axial displacement responses of group B columns.

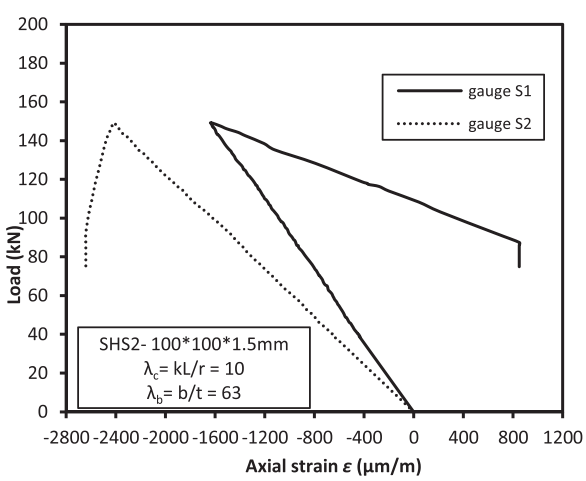

Fig. 21. Load-axial strain responses of control specimen (S100L10T0) of group B.

low values of out-of-straightness and the precision of the test setup alignment. The out-of-straightness has a slight effect compared to the values of measured δ in the opposite direction as shown in Fig. 13 related to LVDT-M1 measurements. In fact, the application process of polymer-mortar layer to the steel column surfaces, using hand lay-up technique, is likely to provide a different pattern of out-of-straightness due to the very unlikely perfect symmetry of the mortar application. It was concluded that polymer-mortar strengthening effectiveness increases for the columns with larger out-of-straightness imperfections and higher slenderness ratios. The lateral displacement of mortar-strengthened specimens decreases compared to those control specimens. The decrease percentage decreases by 69.6%, 53.9%, and 46.7% for mortar-strengthened specimens with *kL/r* of 30, 46, and 58, respectively.

The load versus axial strain (ε) at the two adjacent sides are shown in Fig. 14 related to S2 measurements, and Fig. 15 related to S1 measurements. Both directions were under compression up to a certain load level, at which excessive buckling occurs. It was noted that, the decrease in axial strain of the mortar-strengthened specimens was reduced as the slenderness ratio increases. By carefully examining the strains measured by gauge S2 at failure, it can be noted that higher compressive strains (and hence higher effectiveness) are developed as slenderness ratio *(kL/r)* increases.

3.3. Effect of section's geometry

In this study, two different SHS section's geometries were used. Both SHS1 and SHS2 steel cold-formed sections 80 * 80 mm and 100 * 100 mm with 1.5 mm thick. This means that SHS2 is higher slender than SHS1. According to Stub-column test results, the used two sections SHS1 and SHS2 are approximately similar in yield strength that equal 344 MPa and 327 MPa, respectively. The effect of local buckling on the section capacity of SHS can be investigated by choosing different SHS sections. Certainly, the axial load capacity increased as the section's geometry increases. This can be attributed to higher moment of inertia (*I*) of cross section, and thus increasing the axial strength as anticipated according to Euler's equation. However, the percentage increase in axial strength decreases for higher slender sections (i.e. as the section's geometry increases). Higher slender sections are more prone to the failure where secondary local buckling may or may not occur after overall buckling. The lateral displacement of mortar-strengthened specimens decreases compared to their control specimens as shown in Figs. 16 and 17 related to M2 and M1 measurements, respectively. It was clear that the percentage decrease in lateral displacement seems to be slightly affected by section's geometry.

The percentage decrease in axial strain of the mortar-strengthened specimens increased for higher slender sections as shown in Figs. 18 and 19 related to S2 and S1 measurements, respectively. The axial strain decreases by 40.5%, and 44.5% for 3 mm mortar thickness and to 47.9%, and 56.5% for 6 mm one. In the other direction, the decrease in axial strain was 31.3%, and 36.2% for 3 mm strengthening thickness and to 40.1%, and 48.1% for 6 mm mortar thickness.

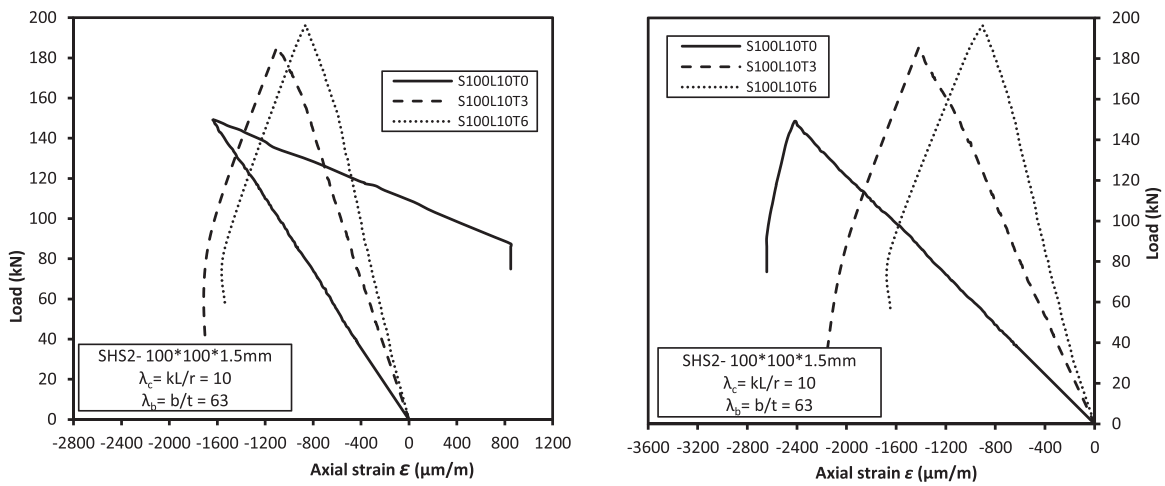

Fig. 22. Load-axial strain responses of group B columns.

3.4. Effect of polymer-mortar strengthening on short columns

Although there are no definite boundaries between short and long columns, it is believed that columns with overall slenderness ratio *(kL/r)* less than 20 may be considered as short columns and will not undergo the overall buckling type of failure, Kulak and Grondin, [3].

In this study, the effect of polymer-mortar thickness on the strength of column was presented. The axial strength of columns increases as the polymer-mortar thickness increases. For group A columns, the gain in strength when increasing the mortar thickness from 3 mm to 6 mm ranged from 8% to 20% for SHS1 and SHS2, respectively. For group B columns, specimen S100L10T6 with 6 mm strengthening thickness achieved the highest gain in axial strength of 31.57%, compared to 24.25% for specimen S100L10T3 strengthened with 3 mm thickness.

The load versus axial displacement curves for all short columns are shown in Fig. 20. The curves are based on the average readings of the three LVDTs mounted on every specimen in a vertical position. The figure shows that, the axial displacement decreases by 56.2%, and 64.4% for mortar-strengthened specimens with mortar thickness of 3 mm, and 6 mm, respectively.

An increase in the compressive strains was observed for control specimen S100L10T0 by both strain gauges S1, and S2 up to peak level, where local buckling took place as shown in Fig. 21. At this level, one side buckles outwards, as indicated by the strains measured by gauge S1, which reverse direction sharply, as a result of the reduction of compressive strain, while the other side buckles inwards, as indicated by gauge S2, which showed increasing compressive strains. Shaat and Fam [14] showed that, although CFRP could brace the two opposite sides that buckle outwards, The CFRP would unlikely have any significant contribution to the sides that buckle inwards which debonds from the steel surface. It is believed that the polymer-mortar could brace both inwards, and outwards sides to completely prevent the local buckling. Fig. 22 also shows the effect of mortar-strengthening system on reducing the axial strain values both inwards, and outwards for all the short columns. The axial strains measured by gauge S1 decreases by 54.8%, and 73.3% for mortar thickness of 3 mm, and 6 mm, respectively. The axial strains measured by gauge S2 decreases by 49.4%, and 64.2% for specimens strengthened with mortar thickness of 3 mm, and 6 mm, respectively.

4. Conclusions

From the results and discussion above, the following conclusions can be made:

- Both the axial strength and stiffness of SHS slender columns are increased using polymer-mortar strengthening materials. The stability of the columns against lateral deflection is improved, and hence, overall buckling occurs at higher loads.
- The effectiveness of the polymer-mortar strengthening system in increasing the axial strength of slender columns increases greatly as the overall slenderness ratio increases. The axial strength of columns with slenderness ratios ranging from 30 to 58 was increased by approximately 39–71%, respectively.
- The axial strength of a column reduces as overall slenderness ratio increases. However, the rate of reduction in mortar-strengthened columns is lower than that of their counterpart bare steel columns.
- The effectiveness of the polymer-mortar strengthening system increases in SHS cold-formed columns with larger out-of straightness imperfections.
- The axial strength of SHS columns increases as the plate slenderness ratio *(b/t)* increases. The percentage increase in axial strength decreases for higher slender sections. The decrease in axial displacement of the mortar-strengthened specimens increases for higher slender sections. However, the decrease in lateral displacement tends to be slightly affected by plate slenderness ratio *(b/t)*.
- Long slender columns fail by excessive overall buckling. In thin-walled sections, this may be followed by secondary local buckling. For slenderness ratios kL/r = 30 and 46, no signs of local buckling or mortar failure by rupture or debonding have been observed. For higher slenderness ratio (kL/r = 58), the secondary local buckling is associated with local debonding and crushing of the mortar strengthening layer at mid-height. The mortar layer on the outer (tension) side remains intact.
- In this study, SHS short columns failed by yielding, immediately followed by symmetric local buckling, where two opposite sides buckled inwards and the other two sides buckled outwards. The polymer-mortar could brace both sides to resist the local buckling.
- Polymer-mortar strengthening system has a great effect on reducing the axial, lateral displacement, and axial strain of the strengthened specimens.

Acknowledgements

Authors are thankful to management and Director of Benha Faculty of Engineering, Benha University, Egypt for rendering the necessary support to carry out this research.

Compliance with ethical standards

Conflict of interests

All authors declare that they have no conflict of interest.

References

[1] ANSI/AISC 360-16, Specification for Structural Steel Buildings, American Institute of Steel Construction, 2016.
[2] CEN.Eurocode 4, Design of Composite Steel and Concrete Structures. Part 1: General Rules and Rules for Building, CEN, Brussels, 2006.
[3] G.L. Kulak, G.Y. Grondin, Limit states design in structural steel, Canadian Institute of Steel Construction, Alliston, Ontario, Canada, 2002.
[4] Jaehong Lee1, Huu Thanh Nguyen2, Seung-Eock Kim2, Buckling and post buckling of thin-walled composite columns with intermediate-stiffened open cross-section under axial compression, Int. J. Steel Struct. 9 (3) (2009) 175–184.
[5] X.L. Zhao, L. Zhang, State-of-the-art review on FRP strengthened steel structures, Eng. Struct. 29 (8) (2007) 1808–1823.
[6] L.C. Hollaway, J. Cadei, Progress in the technique of upgrading metallic structures with advanced polymer composites, Prog. Struct. Eng. Mater. 4 (2) (2002) 131–148.
[7] S. Fawzia, R. Al-Mahaidi, X.L. Zhao, Experimental and finite element analysis of a double lap shear connection between steel plates and CFRP, Compos. Struct. 75 (1–4) (2006) 156–162.
[8] S. Fawzia, M.A. Karim, Investigation into the bond between CFRP and steel plates, World Acad. Sci., Eng. Technol. 53 (2009).
[9] S. Fawzia, R. Al-Mahaidi, X.L. Zhao, Strengthening of circular hollow steel tubular sections using high modulus CFRP sheets, Constr. Build. Mater. 21 (4) (2007) 839–847.
[10] S. Fawzia, X.L. Zhao, R. Al-Mahaidi, S. Rizkalla, "Bond characteristics between CFRP and steel plates in double strap joints", Adv. Steel Constr. – Int. J. 1 (2) (2005) 17–28.
[11] Haider Al-Zubaidy, Riadh Al-Mahaidi, Xiao-Ling Zhao, Experimental investigation of bond characteristics between CFRP fabrics and steel plate joints under impact tensile loads, Compos. Struct. 94 (2012) 510–518.
[12] X.L. Zhao, N.D. Fernando, R. Al-Mahaidi, CFRP strengthened RHS subjected to transverse end bearing force, Eng. Struct. 28 (11) (2006) 1555–1565.
[13] M.R. Bambach, H.H. Jama, M. Elchalakani, Axial capacity and design of thin-walled steel SHS strengthened with CFRP, Thin-Walled Struct. 47 (2009) 1112–1121.
[14] A. Shaat, A. Fam, Axial loading tests on short and long hollow structural steel columns retrofitted using carbon fiber reinforced polymers, Can. J. Civil. Eng. 33 (2006) 458–470.
[15] A. Shaat, A. Fam, "Control of overall buckling of HSS slender steel columns using CFRP plates". in: Smith, S.T. editor. Proceedings of the First Asia-Pacific Conference on FRP in Structures (APFIS 2007). Hong Kong, China, pp. 993–998.
[16] A. Shaat, A. Fam, Fiber-element model for slender HSS columns retrofitted with bonded high- modulus composites, J. Struct. Eng., ASCE 133 (1) (2007) 85–95.
[17] A. Shaat, A. Fam, Strengthening of short HSS steel columns using FRP sheets, Adv. Compos. Mater. Bridges Struct. (2004) 20–23 (ACMBS, Calgary, Alberta, July).
[18] S. El-Tawil, E. Ekiz, Inhibiting steel brace buckling using carbon fiber- reinforced polymers large-scale tests, J. Struct. Eng. 135 (5) (2009) 530–538.
[19] X.D. Liu, A. Nanni, P.F. Silva, Rehabilitation of compression steel members using FRP pipes filled with non-expansive and expansive light-weight concrete, Adv. Struct. Eng. 8 (2) (2005) 129–141.
[20] P. Feng, B. Sawulet, Y.H. Zhang, L.P. Ye, Y. Bai, Experimental study on buckling resistance of steel members strengthened using FRP, Int. J. Struct. Stab. Dyn. 12 (1) (2012) 153–178.
[21] M.A. El Aghoury, A.H. Salema, M.T. Hanna, E.A. Amoush, Strength of cold formed battened columns subjected to eccentric axial compressive force, J. Constr. Steel Res. 113 (2015) (2015) 58–70.